Chapter 1
Climate Change Impacts on Green Water Fluxes in the Eastern Mediterranean

Ibrahim M. Oroud

Abstract The present paper is part of the Glowa Jordan River project, which has been focusing on climate change impacts on environmental, economic and social issues within the lower Jordan river riparian states. The eastern Mediterranean is characterized by scarce and erratic precipitation with relatively cool, wet winters and dry hot summers. Water is the biggest growth-limiting factor. The present paper discusses the use of climate gradient as a tool to examine the impact of climate change on precipitation partitioning over field crops. The present experiment is carried out using a multi-layer, multi-year model with a daily time step. Six years of daily data for five locations, with average annual precipitation ranging from 170 to 580 mm, were used in this investigation. Results show that the ratio of soil evaporation (BE) to annual precipitation (P) during the growing season depends strongly on precipitation regime and amount, ranging from $\sim$15 to 20% when $P > 600$ mm to $\sim$60% when annual $P < 200$ mm. A decrease of 10% in precipitation along with a temperature rise of 2°C increases bare surface evaporation, on average, by $\sim$10% compared to average current conditions. The implications of this would be a tangible reduction in blue and green water fluxes, leading to compulsory land use shift and further water stress in the region.

Keywords Climate change · Mediterranean · Soil moisture partitioning · Rainfed field crops

I. M. Oroud (✉)
Department of Geography, Mu'tah University,
Karak, 61710, Jordan
e-mail: ioroud@mutah.edu.jo

W. Leal Filho (ed.), *Climate Change and the Sustainable Use of Water Resources*,
Climate Change Management, DOI: 10.1007/978-3-642-22266-5_1,

Introduction

Rain-fed field crops are widely grown in western Asia and North Africa. Being located in a transitional zone, this area experiences limited amounts of precipitation with substantial interannual and within season variability. For instance, a 30-year record of precipitation in a station located in this area shows that the average, lowest and highest annual precipitation there were 340, 123 and 639 mm, respectively, with a coefficient of variation of precipitation exceeding 30% in many locations. Precipitation in the eastern Mediterranean exhibits strong spatial gradients both latitudinally and across elevation contour lines. This is clearly depicted in the geographic distribution of water resources, floral composition and dominant agricultural practices.

General circulation models and long-term regional meteorological observations suggest strongly that the eastern Mediterranean will experience a warming trend along with a reduction in annual precipitation during the twenty-first century. This climate change is expected to adversely affect soil moisture availability at different depths, with subsequent impacts on the evapotranspiration regime and biomass production. One of the objectives of this paper is to demonstrate the impact of climate gradient on soil moisture partitioning when planted with a field crop, wheat for instance. The use of climate gradient, or space-for-time approach, provides an assessment of what to expect following a change in climate.

The objective of the present investigation is to examine how soil moisture regime within the active root zone of a wheat crop is influenced by the amount of precipitation and its temporal distribution, and how it is partitioned via direct evaporation and transpiration along a climate gradient. A multi-year, multi-layer simulation model was used. Six years of daily meteorological data for five stations representing the high precipitation zone in Jordan were used in this investigation.

Study Area and Data Quality

The study area represents a semi-dry Mediterranean climate regime with "average" Koppen climate classification of Csa and Csb. The study area is located in the mountainous areas of Jordan, with average annual precipitation ranging from 170 mm to about 550 mm (Fig. 1).

Precipitation falls in the cold season, October/November, and ceases around the end of March/early April. Figure 2 shows the annual course of precipitation in two locations. Annual potential evaporation (PE) in the study area is around 1,000 mm, with the index of aridity ranging from 1.5 in a small mountainous enclave to about 4 in the drier mountainous regions. Six years of continuous daily meteorological data (precipitation, maximum and minimum air temperatures, sunshine hours, cloud cover, wind speed, and ambient vapour pressure) covering the period 1996/1997–2001/2002 were obtained from the Department of Meteorology, Jordan.

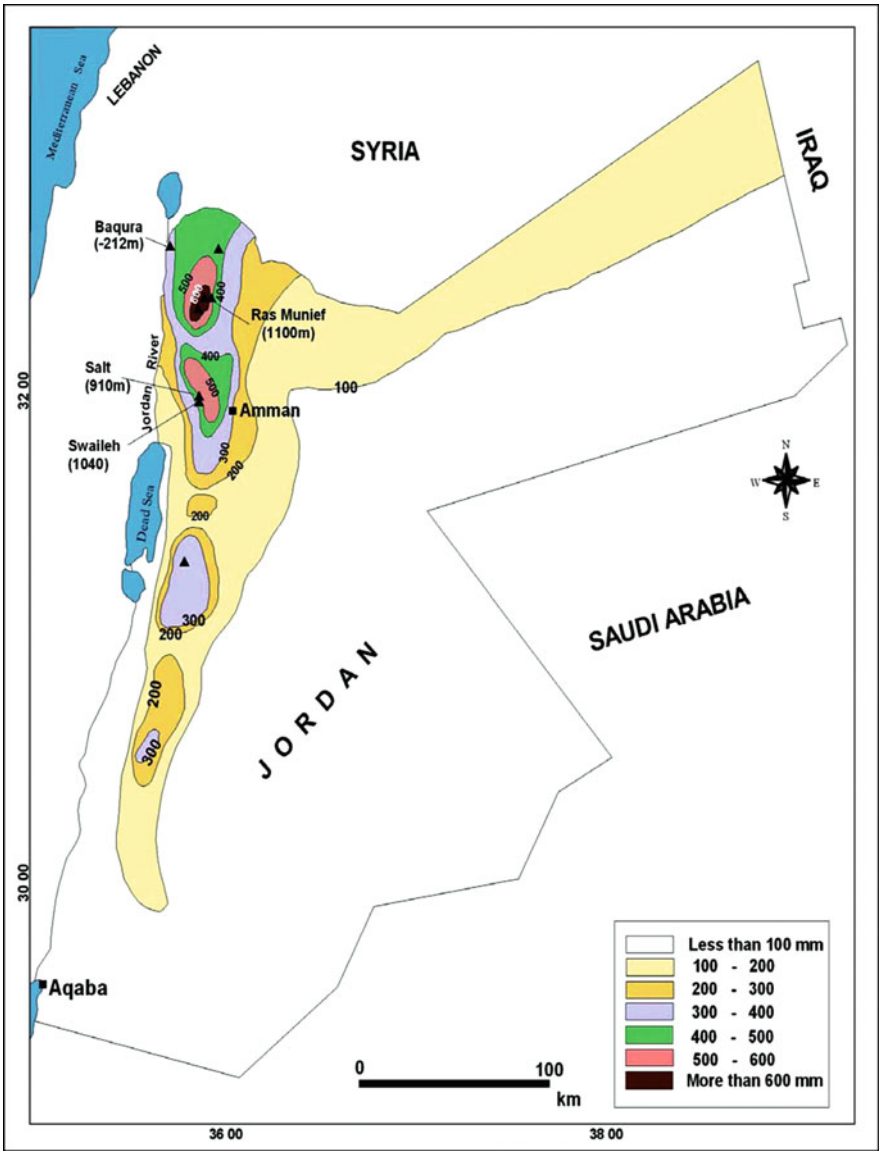

Fig. 1 Location of stations along with elevation (m) and average annual precipitation (mm)

This period covers several growing seasons with wet, average and dry years for the five stations used in the investigation. The selected stations provide good-quality meteorological data with elements being observed on an hourly or three-hourly basis. The data set was quite continuous with few gaps in certain elements which were estimated from neighbouring stations using linear regression, and were checked for consistency.

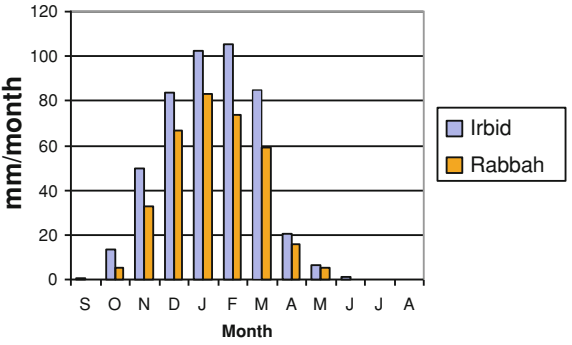

Fig. 2 Monthly distribution of precipitation in two locations, Irbid in northern Jordan and Rabbah in southern Jordan

Method of Investigation

The present investigation is carried out using a cascading water balance model. The water balance of a soil column may be expressed in the following form (e.g. Gleick 1987):

$$\frac{\delta S}{\delta t} = P - BE - A_T - R_O - D_p \tag{1}$$

The first term represents soil moisture change with time; P, BE, A_T, R_O, and D_p are precipitation, bare surface evaporation, actual transpiration, surface runoff, and deep percolation, respectively. In this formulation the soil profile is divided into four equal layers, 0.25 m each, and thus it is assumed that maximum root extension is 1 m. Soil evaporation is determined by atmospheric demand, soil water content, and soil hydraulic properties (e.g. Ritchie 1972).

Atmospheric demand, or PE, is a thermal index which represents the amount of available energy, radiative and advective, that can be used to convert water from its liquid phase into vapour phase. A widely used expression to calculate PE is the Penman–Monteith expression, in which radiative and advective terms were combined to calculate PE (e.g. Dingman 2002).

Actual soil evaporation is either energy-limited or moisture-limited. Most of bare soil evaporation (BE) takes place from layers close to the surface-atmosphere interface. In this formulation, evaporation from the top layer is calculated using the concept of readily available water such that soil evaporation proceeds at its potential rate when skin layer moisture (ω) exceeds atmospheric demands:

$$BE = \tau P_E, \quad \tau P_E \leq \omega, \quad 0 \leq \omega \leq 4 \text{ mm} \tag{2}$$

When skin moisture content does not meet evaporative demands, then direct evaporation is proportional to moisture content of the upper layer,

$$BE = \tau\omega + \tau(P_E - \omega)\left(\frac{\theta_i - \theta_h}{\theta_f - \theta_h}\right)^{1.8}, \quad \tau PE > \omega \tag{3}$$

where BE, P_E, ω, θ_i, θ_h, θ_f, and τ are bare surface evaporation, PE, readily available water for evaporation, actual soil water content, residual water, field capacity, and solar radiation fraction reaching the soil surface, respectively.

The readily available soil water is assumed to be 4 mm. Following rainy events, bare surface evaporation proceeds at its potential rate until ω is less than the potential rate, with Eq. 3 being used instead.

Soil evaporation proceeds only from the top layer when its moisture content is above a threshold value, but when it drops below that, then evaporation proceeds from the deeper layers as well, but with a much reduced rate.

Evaporation/transpiration fraction distribution is assumed to have the following exponential form as suggested by Novak (1987) (see also Zhang et al. 2004),

$$k_\lambda = \frac{D\ \exp(-D(z/z_D))}{z_D(1-\exp(-D))} \tag{4}$$

where D is the water use distribution parameter, and Z_D is the maximum depth that responds to evaporation processes at the surface-atmosphere boundary. The water use distribution parameter for evaporation depends primarily on soil hydraulic properties, and its value may be in the range 6–10 (e.g. Zhang et al. 2004), taken in this paper as 8. When the top layer becomes desiccated, as is the case during the long summer days, evaporation proceeds from the deeper layers.

Surface albedo is parameterized as follows,

$$\alpha = 0.3 - (0.1\tau + 0.04(1-\tau)), \quad 1 < \omega < 4\,\text{mm} \tag{5}$$

$$\alpha = 0.3 - (0.1(\theta/\theta_f)^\beta \tau + 0.04(1-\tau)), \quad \omega < 1\,\text{mm} \tag{6}$$

where ω is skin layer soil moisture wetness factor (taken in this case to be 4 mm), θ and θ_f are the upper surface layer soil moisture and its field capacity, respectively, τ is the fraction of global radiation reaching the ground surface, calculated by (e.g. Oweis et al. 2000; Zhang et al. 2004),

$$\tau = \exp(-K \cdot LAI) \tag{7}$$

where K is solar radiation extinction coefficient, taken in this paper as 0.6 (e.g. Zhang et al. 2004), and LAI is leaf area index. Because of rapid drying of the skin soil layer which determines surface albedo, the exponent β appearing in Eq. 6 is taken as 2.2. Equations 5 and 6 reflect adequately alterations to surface albedo due to upper soil wetting following rainy events and also due to development of foliage coverage.

Soil Moisture and Runoff

Runoff is a function of several parameters (e.g. soil texture and depth, topography, vegetation cover, antecedent soil moisture, precipitation intensity). Because of difficulty in obtaining precipitation intensity, runoff is assumed to be a function of

total daily precipitation (p), soil moisture content of the upper layer (θ_1), and leaf area index (LAI),

$$R_O = f(P, \theta_1, LAI) \tag{8}$$

Runoff may be calculated using the SCS curve. In this formulation, precipitation threshold causing runoff increases as the upper soil layer moisture decreases and as LAI increases. Under such conditions, runoff may occur without the need for the entire soil profile being at its field capacity. The procedure adopted in this paper is similar, in principle, to that presented by Rushton et al. (2006).

Transpiration

The specification of transpiration is crucial for evaluating soil moisture dynamics, leaf area development, and dry matter accumulation, and thus its accurate determination is probably the most significant parameter in this type of study. Transpiration occurs as a result of water potential difference between the soil and plant roots; it is a function of climatic (mainly PE and physiologically active radiation), physiological (LAI, root development and distribution, plant health) and edaphic (soil texture, structure, depth and hydraulic properties) factors (e.g. Brisson 1998; Novak and Havrila 2006). For a well-managed soil, moisture extraction is determined by vertical root extension,

$$A_T = \int_z r(z,t)dz \tag{9}$$

where A_T is actual transpiration and r(z, t) is vertical root distribution. The plant moisture extraction parameter depends on vertical root distribution within the soil layer, and it ranges from 0.5 to about 5 (e.g. Novak 1987; Zhang et al. 2004). The D parameter, presented in Eq. 4, is assigned a value of 1.45 which gives water uptake fractions of 0.41, 0.27, 0.19, and 0.13 for the 0–0.25 m, 0.25–0.5 m, 0.75–0.75 m, and 0.75–1.0 m, respectively. These values are congruent with the widely reported fractions of 0.4, 0.3, 0.2 and 0.1 from the first, second, third and fourth soil layers, respectively (e.g. Gardner 1983). Moisture extraction from each soil layer depends on root extension in each layer and water availability.

Transpiration from a given soil layer is a dynamic parameter which is determined for a well-developed root system by critical leaf water potential and atmospheric forcings (e.g. Nishat et al. 2007). It is assumed that transpiration proceeds at its potential rate when the available moisture in a soil layer exceeds a given threshold level (θ_*), and then decreases linearly until reaching the wilting point (e.g. Hanks 1983; Dingman 2002; Kang et al. 2003),

$$A_T = P_E(1-\tau)\sum_{i}^{n} K_s \cdot y \cdot \gamma_i, \quad \theta_i > \theta_* \tag{10}$$

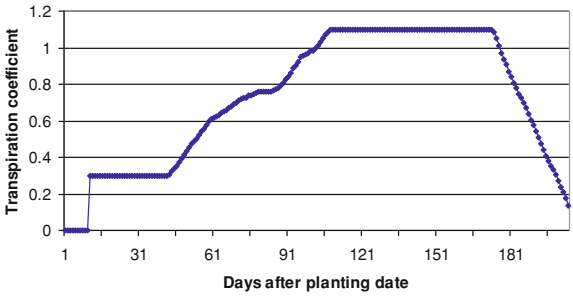

Fig. 3 Simulated transpiration coefficient of winter wheat as a function of plant stage (after Allen et al. 1998)

$$A_T = P_E(1-\tau)\sum_{i}^{n}\frac{\theta_i - \theta_{wp}}{\theta_* - \theta_{wp}}K_s \cdot y \cdot \gamma_i, \quad \theta_i < \theta_* \tag{11}$$

where K_s is the plant transpiration coefficient, which depends on plant stage (Allen et al. 1998), y is the fraction of root extension in the ith soil layer, γ_i is the ith soil layer moisture contribution fraction, and θ_* is the critical soil moisture above which transpiration proceeds at its potential rate. This critical level is influenced primarily by meteorological factors, namely PE; it ranges from values close to 0.8 when atmospheric evaporation demands are high, to values close to the wilting point when evaporative demands are small. The transpiration coefficient was formulated after Allen et al. (1998) for winter wheat crop grown in a Mediterranean environment which ranges from less than 0.2 in late growth stages to 1.1 during the mid growth stage (Fig. 3).

Root vertical development of a cereal crop depends on edaphic elements (e.g. moisture, compaction), weather elements (e.g. PE, growing degree days) and growth stage (e.g. Izzi et al. 2008). Izzi et al. (2008) found that average vertical root growth of wheat in a typical Mediterranean soil in northern Syria is ~ 7 mm/day. In this paper, root growth from seeding to maturity is assumed to be a function of growing degree days. Root vertical growth within a given soil layer, however, depends also on soil water potential. It was indicated that root growth is severely restricted when soil water content is less than ~ -1.0 MPa (e.g. Taylor 1983). In this paper, root vertical extension within the second to fourth layers was not allowed when water content of a layer is less than ~ -1.0 MPa. This occurs during drought-stricken years when precipitation is not sufficient to penetrate to the deeper desiccated soil layers, thereby impeding root development. The germination period is assumed to be 10 days, during which roots are allowed to develop but no leaf development was allowed.

LAI was assumed to be a function of biomass accumulation and senescence. Sowing date was assumed to occur after 25 November, provided that accumulative antecedent precipitation for the period starting from 1 October was at least 40 mm. Farmers tend to plant their land around this time following sufficient amounts of precipitation to ensure germination and subsequent growth for a few weeks to come.

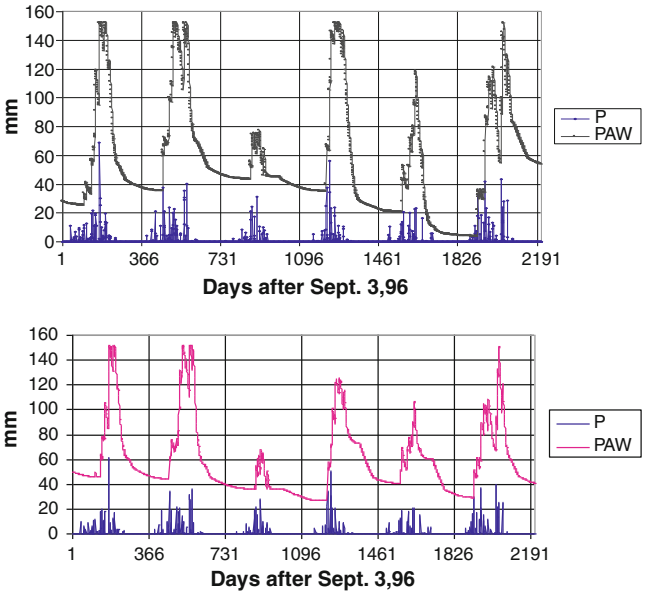

Fig. 4 Plant available water (mm) during the six-year simulation period under current conditions and assuming a 10% precipitation reduction along with a temperature increase of 2°C

Results

Soil Moisture Dynamics

Soil moisture reflects the overall budget of recharge and depletion via evaporation and transpiration due to root-soil moisture differential. Figure 4 shows the annual patterns of precipitation and plant available water (PAW) for the soil profile under current conditions and following a climate change in northern Jordan with average annual precipitation during the study period of 400 mm. There is an annual pattern of soil moisture availability, reaching its maximum during winter and declining during the growing season via both evaporation and root water uptake, and via evaporation during the long dry season. During years with low rainfall, deeper layers are not being replenished, with moisture there being further depleted by evaporation during the following long summer. Long- and short-term drought events are easily detected from moisture curves; poor years are also identified (2000/2001), as the presented moisture curves were narrow and never reached field capacity.

A climate change scenario assuming 2°C temperature increase along with a 10% reduction in precipitation shows that PAW is smaller than under current conditions in all seasons. Although annual patterns are somewhat similar, PAW under climate change scenarios is always less, reflecting the loss of water via direct

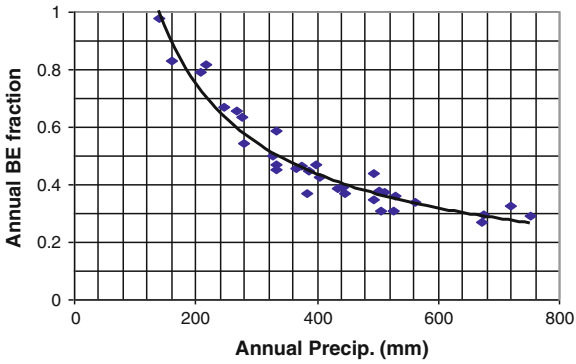

Fig. 5 Annual fraction of direct evaporation from soil for the five stations

evaporation because of the increased evaporative power of the contiguous atmosphere. With an increase of 2°C, annual PE increases by ~12%. The corresponding value for direct surface evaporation (actual) following a climate change is an increase of ~10%. This means that an increase of direct evaporation will come at the expense of blue and green water fluxes. This decrease, although relatively small, is quite significant in this marginal environment, given the very small amount of precipitation in this fragile ecosystem.

Direct Evaporation

Current seasonal direct evaporation ranges, on average, from ~80 mm for drier locations/years to ~120 mm for larger *P* values. The late response of vegetative growth in the mountainous areas, along with frequent surface wetting, intensify direct soil moisture depletion via direct evaporation early in the season.

To demonstrate the impact of climate change on soil moisture dynamics, we used data along a climate gradient. This data set is characterized by substantial interannual and spatial variations. Seasonal bare surface evaporation fraction (BE/P) ranges from ~60% in drier areas/years with annual precipitation <200 mm to ~15–20% when it exceeds ~600 mm. Corbeels et al. (1998) found in a similar environment that direct soil evaporation during the growing season was influenced strongly by precipitation amount, ranging from ~35% in a wet year (P ~400 mm) to ~80% during a dry year (P ~ 260 mm).

Annual soil evaporation fraction in drier realms/years accounts for >90% of total precipitation, whereas in areas/years with more precipitation this fraction is ~25–30% (P > 500 mm). Figure 5 shows the linkage between direct evaporation and precipitation amount for the stations used during the study period.

In drier Mediterranean regions/years, intermittent and scanty precipitation wets the upper soil layer, making it subject to continuous depletion by direct evaporation resulting from large insolation and dry winds following rainy events. Figure 5 demonstrates the steep response of BE to precipitation reduction,

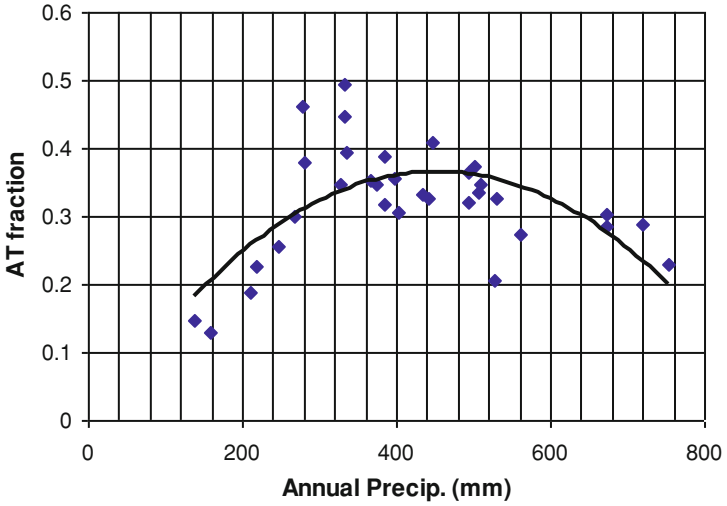

Fig. 6 Transpiration fraction as influenced by seasonal precipitation

particularly at low P values. For instance, a reduction of P from 400 to 360 mm leads to an increase in direct evaporation fraction by $\sim 5\%$, whereas a reduction in annual P from 240 to 200 leads to an increase of BE by $\sim 12\%$.

Transpiration

Transpiration is the most limiting factor in biomass and grain production in dryland farming (e.g. Gardner 1983; Tanner and Sinclair 1983). Wheat is usually sown following sufficient amounts of precipitation. This may occur from mid-November till the end of January. Surface frost occurs frequently in the mountainous areas during the period November to March (Oroud 2007) which, along with low temperatures, slows down vegetative growth. On average, more than 75% of precipitation falls before the end of February, whereas growth begins near the end of February. Figure 6 shows the ratio of wheat transpiration to total crop water demand (potential transpiration) (A_T/P_T) for the five stations during the simulation period. Transpiration fraction reaches its maximum when annual P is between 300 and 500 mm, and then decreases at both ends of precipitation. When P is small, soil moisture is lost via direct evaporation, and at large P values, it is lost as blue water.

Discussion

The concept of climate gradient as represented by interannual precipitation variability for a total of 30 years provides a measure of soil moisture dynamics and how precipitation is partitioned via various avenues. The present method provides

realistic representations of precipitation partitioning via various avenues. Surface evaporation proceeds at its potential following rainy events until the wetness fraction drops below a critical level and then it continues at a reduced rate. Unlike other methods which deal with surface albedo as a constant, the present paper treats this element dynamically such that it changes following wetting/drying episodes and also in response to foliage development. This treatment is important given the fact that a change in surface albedo influences water loss appreciably following rainy events. Following rainy events, net radiation increases as a result of surface temperatures reduction and suppressed albedo due to strong spectral absorption ($\lambda > 0.75$ μm). The combined effects of increased global radiation along with a reduced albedo due to surface wetting enhance direct evaporation from soils. A 5% difference in surface albedo leads to $\sim$12–15% difference in net radiation, and correspondingly a similar evapotranspiration difference. This is important following rainy events, as actual evapotranspiration is energy-limited following these events.

The meagre amount of precipitation, which usually wets the top soil layer, along with substantial evaporative demands, enhances direct evaporation in this environment. Results show that bare surface evaporation represents a significant fraction of precipitation for areas receiving less than 300 mm of annual precipitation, with a total annual fraction exceeding 90% in these areas. These results are congruent with those presented by Zhang et al. (1998), Oweis et al. (2000) in northern Syria, Corbeels et al. (1998) in Morocco, and Monzon et al. (2006) in southwestern Australia where Mediterranean-like conditions prevail. With a climate change, drought frequency and severity will be more intense in the near future compared to those experienced during the twentieth century. Under such conditions, traditional areas which sustained dry agriculture practices during the Holocene will be less suitable for rain-fed agriculture, with more frequent crop failure. Although people and decision-makers will continue denying these environmental changes, more intense drought episodes and frequent crop failures will force these new painful realities. Consequently, a shift in land use from agricultural towards grazing is an inevitable outcome of a climate change in this fragile habitat.

Conclusion

A simulation model with a daily time step is developed to examine the partitioning of precipitation along a climate gradient. Results show that direct evaporation represents the largest water loss component in areas receiving less than 300 mm of annual precipitation. The substantial evaporation fraction in dry areas indicates clearly that rainwater harvesting (deep trenches for underground recharge or small-scale collection systems directed to enhance green water fluxes) is the best available option to conserve water and to maximize its usefulness in these marginal areas.

Acknowledgments This paper is part of the GLOWA Jordan River Project Phase 3 which is funded by BMBF, Germany.

References

Allen RG, Pereira LS, Raes D, Smith M (1998) Crop evapotranspiration guidelines for computing crop water requirements. FAO irrigation and drainage paper 56, FAO, Rome

Brisson N (1998) An analytical solution for the estimation of the critical available soil water fraction for a single layer water balance model under growing crops. Hydrol Earth Sys Sci 2:221–231

Corbeels M, Hofmann G, van Cleemput O (1998) Analysis of water use by wheat grown on a cracking clay soil in a semi-arid Mediterranean environment: weather and nitrogen effects. Agric Water Manage 38:147–167

Dingman SL (2002) Physical Hydrology, 2nd edn. Prentice Hall, New Jersey

Gardner WR (1983) Soil properties and efficient water use: an overview. In: Taylor H, Jordan W, Sinclair TR (eds) Limitations to efficient water use. American Society of Agronomy, Inc., USA

Gleick PH (1987) The development and testing of a water balance model for climate impact assessment: modeling the Sacramento basin. Water Resour Res 23:1049–1061

Hanks RJ (1983) Yield and water-use relationship: an overview. In: Taylor H, Jordan W, Sinclair TR (eds) Limitations to efficient water use. American Society of Agronomy, Inc., USA

Izzi G, Farahani HJ, Bruggeman A, Oweis TY (2008) In-season wheat root growth and soil water extraction in the Mediterranean environment of northern Syria. Agric Water Manage 95:259–270

Kang S, Gu B, Du T, Zhang J (2003) Crop coefficient and ratio of transpiration to evapotranspiration of winter wheat and maize in a semi-*'humid'* region. Agric Water Manage 59:230–254

Monzon JP, Sadras VO, Andrade FH (2006) Fallow soil evaporation and water storage as affected by stubble in sub-humid (Argentina) and semi-arid (Australia) environments. Field Crops Res 98:83–90

Nishat S, Guo Y, Baetz BW (2007) Development of a simplified continuous simulation model for investigating long term soil moisture. Agric Water Manage 92:53–63

Novak V (1987) Estimation of soil water extraction patterns by roots. Agric Water Manage 12:271–278

Novak V, Havrila J (2006) Method to estimate the critical soil water content of limited availability for plants. Biol Bratisl 61(Suppl 19):S289–S293

Oroud IM (2007) Spatial and temporal distribution of frost in Jordan. Arab World Geogr 10:81–91

Oweis T, Zhang H, Pala M (2000) Water use efficiency of irrigated bread wheat in a Mediterranean environment. Agron J 92:231–238

Ritchie J (1972) Model for predicting evaporation from a row crop with incomplete cover. Water Resour Res 8:1204–1213

Rushton KR, Eiler VHM, Carter RC (2006) Improved soil moisture balance methodology for recharge estimation. J Hydrol 318:379–399

Tanner CB, Sinclair TR (1983) Efficient water use in crop production. In: Taylor H, Jordan W, Sinclair TR (eds) Limitations to efficient water use. American Society of Agronomy, Inc., USA

Taylor HM (1983) Managing root system for efficient water use: an overview. In: Taylor H, Jordan W, Sinclair TR (eds) Limitations to efficient water use. American Society of Agronomy, Inc., USA

Zhang H, Oweis TY, Garabet S, Mustafa P (1998) Water-use efficiency and transpiration efficiency of wheat under rain-fed conditions and supplemental irrigation in a Mediterranean-type environment. Plant Soil 201:295–305

Zhang Y, Yu Z, Liu C, Jiang L, Zhang X (2004) Estimation of winter wheat evapotranspiration under water stress with two semi-empirical approaches. Agron J 96:159–168